Inseparable Time-Crystal Geometries on the Möbius Strip

Krzysztof Giergiel,[1] Arkadiusz Kuroś,[1,3] Arkadiusz Kosior,[1,2,4] and Krzysztof Sacha[1]
[1]Instytut Fizyki Teoretycznej, Uniwersytet Jagielloński, ulica Profesora Stanisława Łojasiewicza 11, PL-30-348 Kraków, Poland
[2]Max-Planck-Institut für Physik Komplexer Systeme, Nöthnitzer Strasse 38, D-01187 Dresden, Germany
[3]Institute of Physics, Jan Kochanowski University, ul. Uniwersytecka 7, 25-406, Kielce, Poland
[4]Institute for Theoretical Physics, University of Innsbruck, 6020 Innsbruck, Austria

(Received 22 March 2021; accepted 24 November 2021; published 22 December 2021)

Description of periodically and resonantly driven quantum systems can lead to solid state models where condensed matter phenomena can be investigated in time lattices formed by periodically evolving Wannier-like states. Here, we show that inseparable two-dimensional time lattices with the Möbius strip geometry can be realized for ultracold atoms bouncing between two periodically oscillating mirrors. Effective interactions between atoms loaded to a lattice can be long-ranged and can be controlled experimentally. As a specific example, we show how to realize a Lieb lattice model with a flat band and how to control long-range hopping of pairs of atoms in the model.

DOI: 10.1103/PhysRevLett.127.263003

Introduction.—In the last few decades, engineering of elaborate optical potentials has been a prominent subject of both theoretical and experimental research in ultracold atoms [1,2]. Recent experimental techniques enable not only creation of periodic optical potentials of various geometries [3,4] but also manipulation of parameters of the effective models and introduction of artificial gauge fields [5]. The latter allows one to realize topologically nontrivial energy bands, which are the cornerstone of topological insulators and quantum Hall systems [6]. The real space topology proves to be equally important—for example, it has been shown that global properties of spinless particles on the Möbius ladder can be locally described by a non-Abelian gauge potential [7,8] and that the quantum Hall effect is forbidden on nonorientable surfaces [9]. Unfortunately, realization of nontrivial real space topologies can be challenging. Although it has been shown that topologically nontrivial one-dimensional ladder geometries can be implemented by using a synthetic dimension [10,11], higher dimensional systems have remained elusive so far.

On the other hand, recently there has been an increasing number of theoretical works on time crystals [12–41], followed by experimental demonstrations [42–51] and modeling of crystalline structures in periodically driven systems [52–57] (for reviews see [58–61]). The latter opens a path to realization of temporal analogs of condensed matter physics and exploration of novel phenomena present exclusively in the time dimension. In particular, in this Letter we show the construction of two-dimensional inseparable time lattices that naturally entails the Möbius strip geometry. Specifically, we identify reduction of the description of atoms resonantly bouncing between two periodically oscillating mirrors to the tight-binding Hamiltonian, where particles can tunnel between localized Wannier-like wave packets that evolve periodically along classical resonant trajectories. The crystalline structure corresponding to the tight-binding Hamiltonian can be observed not in space but in the time domain. That is, if we locate a particle detector close to a resonant trajectory, the dependence of the probability of clicking of the detector as a function of time reproduces a cut of the crystalline structure described by the model [61]. This reflects the fact that, in time crystals, the roles of time and space are interchanged.

In the following, we show how to realize tight-binding models on a two-dimensional (2D) crystalline structure on the Möbius strip in the time domain. We propose a universal setup where the emergent lattice geometry can be shaped almost at will depending on the driving protocol of the mirrors. As a particular example, we choose the Lieb lattice with a flat band [62–66] where dynamics of atoms is governed solely by interactions. We stress that the effective interactions of the model are long-ranged and can be experimentally controlled. This creates a unique platform to study exotic flat band many-body physics. In the next sections, we describe the main elements of the theoretical approach, leaving the details for [67].

Möbius strip geometry.—Let us start with a classical particle bouncing between two static mirrors located at $x = 0$ and $x - y = 0$, which form a wedge with the angle 45° (Fig. 1). In the gravitational units [68,69], the Hamiltonian reads $H_0 = (p_x^2 + p_y^2)/2 + x + y$ with the constraint $y \geq x \geq 0$ coming from the hard wall potential of the mirrors (for a Gaussian shaped mirror potential see [39]). When a particle collides with the vertical mirror, its momenta are exchanged $p_x \leftrightarrows p_y$, whereas when a particle hits the other mirror, p_y remains the same but $p_x \to -p_x$; see Fig. 1.

To find how to describe a particle confined in the wedge with the angle 45°, one can start with the problem of

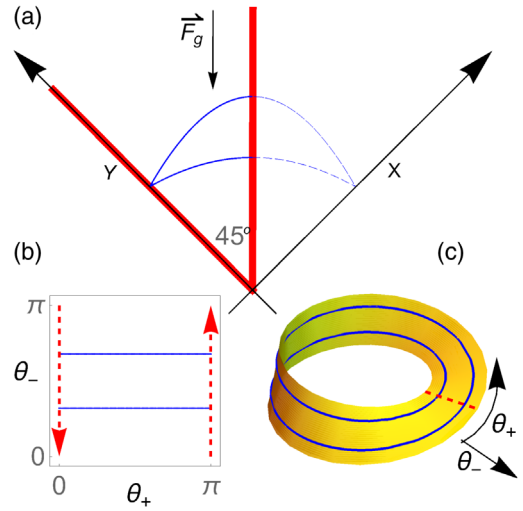

FIG. 1. (a) A geometry of the system where a particle in the presence of the gravitational force $\vec{F}_g$ is bouncing between two mirrors (thick red lines) forming a 45° wedge. (b) If the mirrors do not oscillate, a set of trajectories (a sample trajectory shown in blue) corresponding to equal energies $E_x = E_y$ cover a region with $\theta_\pm \in [0, \pi)$. In a collision with the vertical mirror, i.e., at $\theta_+ = \pi$, the momenta components of a particle are exchanged, which reverses the direction of the momentum vector $p_{x,y} \to -p_{x,y}$ because for $E_x = E_y$ we have $p_x = -p_y$. This results in $\theta_\pm \to \pi - \theta_\pm$. These conditions identify points $\{\theta_+ = \pi, \theta_-\} = \{\theta_+ = 0, \pi - \theta_-\}$ and define the Möbius strip geometry (c).

two perpendicular mirrors. When the angle between two mirrors is 90°, the system is separable in the Cartesian coordinate frame [70,71] and it is convenient to switch to the action-angle variables I_α and θ_α with $\alpha = x, y$. Then, the Hamiltonian H_0 depends on the actions I_α only [72,73]. The dynamics of the angles is given by Hamilton's equations $\dot{\theta}_\alpha = \partial H_0/\partial I_\alpha \equiv \Omega_\alpha(I_\alpha)$, where $\Omega_\alpha(I_\alpha)$ are frequencies of motion along the x and y directions. Since the actions I_α are constants of motion, the solution for the angles is trivial: $\theta_\alpha(t) = \Omega_\alpha(I_\alpha)t + \theta_\alpha(0)(\mathrm{mod}\ 2\pi)$. Motion of a particle is confined on a surface of a two-dimensional torus. In this Letter, we consider periodic trajectories of a particle that are symmetric with respect to the vertical mirror. It implies that the initial conditions correspond to equal energies of the x and y degrees of freedom, i.e., $E_x = E_y$ (or $I_x = I_y$) and thus $\Omega_x(I_x) = \Omega_y(I_y)$. To reduce the number of frequencies, we perform a canonical transformation from $(I_\alpha, \theta_\alpha)$ to new variables $I_\pm = I_y \pm I_x$ and $\theta_\pm = (\theta_y \pm \theta_x)/2$ [67]. The equations of motion in such variables have the form $\dot{I}_\pm = 0$, $\dot{\theta}_- = 0$, and $\dot{\theta}_+ = \Omega_+(I_+)$, where $I_- = 0$ and the value of the action I_+ determines the frequency of a periodic orbit [74]. Thus, $\theta_+(t) = \Omega_+(I_+)t + \theta_+(0)$ describes motion along a periodic orbit while θ_- is a constant.

Let us come back to the wedge with the angle 45°, where the motion is restricted to $y \geq x$ (or equivalently $0 < \theta_+ \leq \pi$). When a particle bounces off a vertical mirror, the momenta are exchanged $p_x \leftrightarrows p_y$. For $E_x = E_y$, we have $p_x = -p_y$ and therefore $p_\alpha \to -p_\alpha$ at $y = x$, or, in other words, $\theta_\pm \to \pi - \theta_\pm$ at $\theta_+ = \pi$. The latter identifies points $\{\theta_+ = \pi, \theta_-\} = \{\theta_+ = 0, \pi - \theta_-\}$ and defines the Möbius strip geometry (see Fig. 1). In order to realize condensed matter physics on the Möbius strip, oscillations of the mirrors will be turned on. We will see that resonant bouncing of a single atom or a cloud of atoms between the oscillating mirrors can be described by solid state models. The emerging crystalline structures will be observed not in space but in the time domain.

Oscillating mirrors.—Let us assume that the mirror located around $x = 0$ oscillates in time like $f_x(t) = -(\lambda_1/\omega^2)\cos(\omega t) - (\lambda_2/4\omega^2)\cos(2\omega t)$, while the vertical one like $f_{y-x}(t) = (\lambda_3/4\omega^2)\cos(2\omega t + \phi)$, where $\lambda_{1,2,3}$ are amplitudes and ϕ is a constant phase. It is convenient to switch to the frame oscillating with the mirrors. Then, the mirrors are static, and the Hamiltonian of an atom reads $H = H_0 + (x + y)f_x''(t) + yf_{y-x}''(t)$; see [67]. We focus on the resonant driving of an atom where the frequency ω of the oscillations of the mirrors fulfills the s:1 resonant condition, i.e., $\omega = s\Omega_+(I_+^0)$, where s is an integer number, I_+^0 is the resonant value of the action I_+, and $I_- = I_-^0 = 0$.

In order to describe classical motion of an atom close to resonant trajectories, one may apply the secular approximation approach, which in the action-angle variables and in the moving frame $\Theta_+ = \theta_+ - \omega t/s$ and $\Theta_- = \theta_-$ leads to the following effective Hamiltonian [67]:

$$H_{\mathrm{eff}} = -\frac{P_-^2 + P_+^2}{2|m_{\mathrm{eff}}|} - \frac{\lambda_2}{2\omega^2}\cos(2s\Theta_+)\cos(2s\Theta_-) - \frac{2\lambda_1}{\omega^2}\cos(s\Theta_+)\cos(s\Theta_-) + \frac{\lambda_3}{4\omega^2}\cos(2s\Theta_+ + \phi), \tag{1}$$

where $P_\pm = I_\pm - I_\pm^0$ and $|m_{\mathrm{eff}}| = (3I_{0+})^{4/3}/(2\pi^2)^{1/3}$. The Eq. (1) Hamiltonian describes a particle with the negative effective mass $-|m_{\mathrm{eff}}|$ in the presence of an inseparable lattice potential that is moving on the Möbius strip because at $\Theta_+ = \pi$ there are the flips $\Theta_\pm \to \pi - \Theta_\pm$. Different parameters of the mirrors' oscillations allow one to realize different crystalline structures of the effective potential in Eq. (1). For example, for $\lambda_3/\lambda_1 = 4$, $\lambda_2 = 0$ and $\phi = 0$, a honeycomb lattice [3,4] can be realized [Fig. 2(a)], while for $\lambda_2/\lambda_1 = 4$, $\lambda_3/\lambda_2 = 1.62$ and $\phi = \pi/4$, the Lieb lattice with a flat band emerges [Fig. 2(b)]. In the following, we focus on the Lieb lattice case as a concrete example.

To obtain a quantum description of a particle resonantly bouncing between the mirrors, one can either quantize the classical Hamiltonian [Eq. (1)], i.e., replace $P_\pm \to -i\partial/\partial\Theta_\pm$, or apply the fully quantum secular approximation method for the Floquet Hamiltonian $H_F = H - i\partial_t$ (see [67]). The former is very useful to understand what kind of effective behavior we can expect. The latter is a

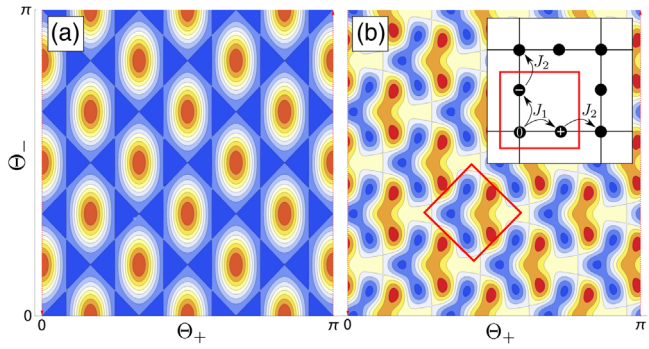

FIG. 2. Examples of the effective potential in Eq. (1). Dark blue color represents areas around maxima of the effective potential that correspond to the lowest energies of H_{eff} for a particle with a negative effective mass. The geometry of the $\{\Theta_+, \Theta_-\}$ space is the Möbius strip geometry as in Fig. 1. (a) The effective potential for $\lambda_3/\lambda_1 = 4$, $\lambda_2 = 0$, and $\phi = 0$ creates a honeycomb lattice structure. (b) Maxima of the effective potential for $\lambda_2/\lambda_1 = 4$, $\lambda_3/\lambda_2 = 1.62$, and $\phi = \pi/4$ correspond to the Lieb lattice with a well separated central flat band. A unit cell (red square) of the Lieb lattice is composed of three sites. Inset: A tunneling structure in the Lieb lattice.

more systematic quantum description that allows one to easily incorporate the boundary conditions on the mirrors and particle interactions, and we use it to obtain all quantum results shown in this Letter. These two quantum approaches agree very well with each other if $I_+^0 \gg 1$.

We concentrate on an example where the effective potential in the Eq. (1) Hamiltonian correspond to the Lieb lattice [Fig. 2(b)]. The Lieb lattice is a Bravais lattice with a three point basis, and therefore the lattice sites can be labeled by a unit cell index j and an intra cell index $\beta = 0, \pm$; see Fig. 2(b). Description of the first energy manifold of the effective Hamiltonian can be reduced to the tight-binding model

$$H_F \approx -J_1 \sum_{i,\beta=\pm} \hat{a}_{i,0}^\dagger \hat{a}_{i,\beta} - J_2 \sum_{\langle ij\rangle,\beta=\pm} \hat{a}_{i,0}^\dagger \hat{a}_{j,\beta} + \mathrm{H.c.}, \quad (2)$$

where $\hat{a}_{i,\beta}/\hat{a}_{i,\beta}^\dagger$ are bosonic operators that annihilate or create a particle in the Wannier states $W_{i,\beta}(\Theta_+, \Theta_-)$. J_1 and J_2 are intra- and intercell tunneling amplitudes, respectively, cf. Fig. 2(b). As long as $J_1 \neq J_2$, eigenvalues of Eq. (2) form three separated bands, where the central one is flat [66,67]. In the flat band, the group velocity is zero and consequently the transport in the flat band is totally halted unless we deal with a many-body system with interactions.

The Eq. (1) Hamiltonian indicates that in the moving frame we deal with a crystalline structure in the $\{\Theta_+, \Theta_-\}$ space. In the tight-binding approximation [Eq. (2)], eigenstates of an atom are superposition of the Wannier states $\psi(\Theta_+, \Theta_-) = \sum_{i,\beta} c_{i,\beta} W_{i,\beta}(\Theta_+, \Theta_-)$. When we return to the laboratory frame, no crystalline structure is observed in the Cartesian coordinates x and y. However, if a detector is located close to a resonant trajectory (i.e., we fix θ_+ and θ_- and $I_\pm \approx I_\pm^0$), then the dependence of the probability of clicking of the detector as a function of time reproduces a cut of the probability density in the $\{\Theta_+, \Theta_-\}$ space, i.e., $|\psi(\Theta_+, \Theta_-)|^2 = |\psi(\theta_+ - \omega t/s, \theta_-)|^2$. Different locations of the detector (different $\theta_\pm$) correspond to different cuts of the crystalline structure in the $\{\Theta_+, \Theta_-\}$ space. Note that such a crystalline structure in time is not a result of spontaneous breaking of time translation symmetry. It is a time lattice that emerges in the dynamics of the system due to the external driving like in the case of photonic crystals, which do not form spontaneously because periodic modulation of the refractive index in space has to be imposed externally.

Quantum many-body physics in the flat band.—In the previous paragraphs, we have shown how to realize an effective potential in the $\{\Theta_+, \Theta_-\}$ space, where a localized particle tunnels between the Wannier states $W_{j,\beta}(\Theta_+, \Theta_-)$ centered at the sites of the Lieb lattice [Eq. (2)]. The eigenstates of the flat band can be chosen as the maximally localized Wannier states w_j. For $J_1/J_2 \gg 1$, the Wannier states w_j spanning the flat band can be approximated by superpositions of two localized wave packets, $w_j \approx (W_{j,+} - W_{j,-})/\sqrt{2}$, for the bulk states or $w_j \approx W_{j,\pm}$ for the states close to the edge of the Möbius strip [75]; see Fig. 3.

Hopping of bosons in the flat band can only happen if there are interactions between them. In ultracold atoms, the interactions are zero-range and we assume that interaction energy per particle is much smaller than the energy gaps between the flat and adjacent bands. Then, we may still restrict to the flat band only and the effective many-body Floquet Hamiltonian reads [61]

$$\begin{aligned} H_F &= \frac{1}{sT}\int_0^{sT} dt \int dxdy \hat{\psi}^\dagger \left(H - i\partial_t + \frac{g_0}{2}\hat{\psi}^\dagger\hat{\psi}\right)\hat{\psi} \\ &\approx \sum_{ijkl} U_{ijkl} \hat{b}_i^\dagger \hat{b}_j^\dagger \hat{b}_k \hat{b}_l + \mathrm{const}, \end{aligned} \quad (3)$$

where H is the single particle Hamiltonian $\hat{\psi} \approx \sum_{i=1}^{s(s+1)/2} w_i \hat{b}_i$ with the bosonic operators $[\hat{b}_i, \hat{b}_j^\dagger] = \delta_{ij}$, and $U_{ijkl} = (sT)^{-1} \int dt g_0 u_{ijkl}(t)$ with

$$u_{ijkl}(t) = \int dxdy w_i^* w_j^* w_k w_l. \quad (4)$$

In the laboratory frame, the Wannier states $w_i(x, y, t)$ of the flat band are superpositions of localized wave packets evolving periodically with the period sT. Indices $i, j, \ldots$ label sites of the effective square lattice that correspond to a unit cell index of the Lieb lattice, cf. Fig. 3. In the course of time evolution, different localized wave packets can overlap in the laboratory frame at different moments of time. The strength g_0 of the atom-atom interactions depends

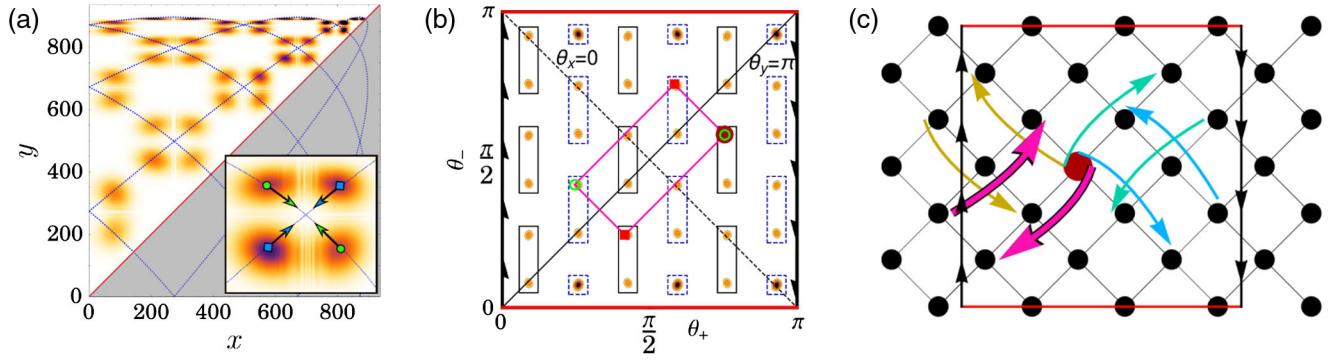

FIG. 3. (a) Probability density (in the lab frame and in the Cartesian coordinates at $t = \omega\pi/5$) of the Wannier states w_i belonging to the flat band of the effective Lieb lattice potential, cf. Fig. 2(b). Inset: An enlargement of four encountering localized wave packets belonging to four different Wannier states: w_i, w_j, w_k, w_l. (b) Same as in (a) but in the $\{\theta_+, \theta_-\}$ space. The Wannier states, enclosed by rectangles, are either superpositions of two localized wave packets or just a single one at the edge of the Möbius strip. In the course of time evolution, the entire structure is moving uniformly along the θ_+ axis and fulfills the Möbius strip boundary conditions. (c) The hopping structure of the effective lattice of the flat band, where black dots correspond to the Wannier states w_i, and arrows of the same color indicate hoppings of atomic pairs. The horizontal direction of the lattice is related to the direction along the Möbius strip, cf. Fig. 1(c). Note that for illustrative purposes we have only shown the hoppings along the smallest symmetric rectangles [cf. panel (b)] that involve annihilation of one atom in a central (brown) site. Panels correspond to $s = 6$, $\omega = 0.315$, $\lambda_1 = 2.48 \times 10^{-4}$, $\lambda_2 = 9.9 \times 10^{-4}$, $\lambda_3 = 1.61 \times 10^{-3}$, and $\phi = \pi/4$ in Eq. (1).

on the s-wave scattering length and can be controlled by means of the Feshbach resonance [76]. Suppose that g_0 is periodically modulated in time, i.e., $g_0(t) = g_0(t + sT)$. The interaction strength $g_0(t)$ can be turned on only for a moment of time when specific Wannier states overlap in the laboratory frame. Thus, we can engineer the interaction coefficients U_{ijkl} in the flat band system, Eq. (3), almost at will, which allows one to explore different exotic flat band models. Let us analyze what kinds of models are attainable in the flat band of the Lieb lattice potential presented in Fig. 2(b).

Even if localized wave packets belonging to Wannier states w_i, w_j, w_k, and w_l overlap in the laboratory frame at a certain moment of time, it does not necessarily mean that the corresponding $u_{ijkl}(t)$ in Eq. (4) is not zero. An atom that occupies a localized wave packet is characterized by a quite well defined momentum and if the sum of the momenta of two atoms before and after a collision at t is not conserved, the corresponding $u_{ijkl}(t)$ vanishes. If, however, $u_{ijkl}(t)$ does not vanish at a certain time moment t, then we can get the value of the interaction coefficient U_{ijkl} as we wish by choosing an appropriate $g_0(t)$. In the case of the flat band of the Lieb lattice presented in Fig. 2(b), effective selection rules for nonvanishing $u_{ijkl}(t)$ are illustrated in Fig. 3(b). Corners of a symmetrically located rectangle in Fig. 3(b) correspond to the same position in the Cartesian space $\{x, y\}$ but to four different pairs of the momenta $\{\pm p_x, \pm p_y\}$ [67]. If at a certain t four localized wave packets are at the corners of a certain symmetric rectangle, then we have a guarantee that $u_{ijkl}(t)$ does not vanish, which enables simultaneous hopping of two atoms on the Lieb lattice. Note that two wave packets corresponding to the same Wannier state are not necessarily neighbors in the laboratory frame.

To sum up, apart from the simultaneous hopping of pairs of atoms described in Fig. 3, on-site and long-range density-density interactions can be present in the flat band, but no density induced tunneling is allowed. Taking into account all possible processes, a general many-body effective Floquet Hamiltonian in the flat band becomes

$$H_F = \sum_i U_i \hat{n}_i(\hat{n}_i - 1) - \sum_{\{ijkl\}} J_{ijkl} \hat{b}_i^\dagger \hat{b}_j^\dagger \hat{b}_k \hat{b}_l, \qquad (5)$$

where $\hat{n}_i = \hat{b}_i^\dagger \hat{b}_i$. The first sum describes the on-site interactions with the coupling strengths $U_i = U_{iiii}$, while the second sum, with terms proportional to $J_{ijkl} = 4U_{ijkl}|_{i \neq j}$, is responsible for the long-range density-density interactions and the simultaneous hopping of pairs of atoms. In Fig. 3(c), we illustrate simultaneous hopping of atoms by only two lattice sites, and other possible kinds of hopping are shown in [67]. Studies of many-body phases of the Lieb model we describe here is beyond the scope of this Letter.

Conclusions.—In this Letter, we show that a very simple setting of two oscillating mirrors has a potential for realization of nonequilibrium many-body physics on inseparable lattices with the Möbius strip geometry. Our system reduces to a time lattice where localized wave packets are moving along classical resonant orbits. By controlling the periodic motion of the mirrors, one is able to design arbitrary lattice geometries. We argue that the effective interactions of the model can be exotic, long-ranged, and experimentally tunable. In order to emphasize these peculiar features, we focus on a flat band of the Lieb

lattice with interaction induced long-distance simultaneous hoppings of atomic pairs. Another unique property of our construction is that the 2D time crystalline structures have the geometry of the Möbius strip. It is known that the lack of translational symmetry of the Möbius strip can change the ground state and low energy physics properties of many-body models [10]. Therefore, our results not only open up new perspectives for the exploration of interaction induced phenomena, such as exotic superfluids and supersolids on a flat band or the strongly correlated constrained dynamics in the strongly interacting models, but also enable the study of topological effects due to the nontrivial lattice geometry.

K. G. and A. Kuroś contributed equally to the present work. This work was supported by the National Science Centre, Poland via Projects No. 2016/20/W/ST4/00314 and No. 2019/32/T/ST2/00413 (KG), QuantERA Program No. 2017/25/Z/ST2/03027 (A. Kuroś), No. 2018/31/B/ST2/00349 (A. Kosior and K. S.). K. G. acknowledges the support of the Foundation for Polish Science (FNP).

[1] M. Lewenstein, A. Sanpera, and V. Ahufinger, *Ultracold Atoms in Optical Lattices: Simulating Quantum Many-body Systems* (Oxford University Press, New York, 2017), ISBN 9780198785804, https://books.google.pl/books?id=JsebjwEACAAJ.
[2] A. Eckardt, Rev. Mod. Phys. **89**, 011004 (2017).
[3] L. Tarruell, D. Greif, T. Uehlinger, G. Jotzu, and T. Esslinger, Nature (London) **483**, 302 (2012).
[4] P. Windpassinger and K. Sengstock, Rep. Prog. Phys. **76**, 086401 (2013).
[5] N. Goldman, G. Juzeliunas, P. Öhberg, and I. B. Spielman, Rep. Prog. Phys. **77**, 126401 (2014).
[6] M. Z. Hasan and C. L. Kane, Rev. Mod. Phys. **82**, 3045 (2010).
[7] Z. L. Guo, Z. R. Gong, H. Dong, and C. P. Sun, Phys. Rev. B **80**, 195310 (2009).
[8] N. Zhao, H. Dong, S. Yang, and C. P. Sun, Phys. Rev. B **79**, 125440 (2009).
[9] W. Beugeling, A. Quelle, and C. Morais Smith, Phys. Rev. B **89**, 235112 (2014).
[10] O. Boada, A. Celi, J. I. Latorre, and M. Lewenstein, Phys. Rev. Lett. **108**, 133001 (2012).
[11] O. Boada, A. Celi, J. Rodríguez-Laguna, J. I. Latorre, and M. Lewenstein, New J. Phys. **17**, 045007 (2015).
[12] F. Wilczek, Phys. Rev. Lett. **109**, 160401 (2012).
[13] K. Sacha, Phys. Rev. A **91**, 033617 (2015).
[14] V. Khemani, A. Lazarides, R. Moessner, and S. L. Sondhi, Phys. Rev. Lett. **116**, 250401 (2016).
[15] D. V. Else, B. Bauer, and C. Nayak, Phys. Rev. Lett. **117**, 090402 (2016).
[16] N. Y. Yao, A. C. Potter, I.-D. Potirniche, and A. Vishwanath, Phys. Rev. Lett. **118**, 030401 (2017).
[17] A. Lazarides and R. Moessner, Phys. Rev. B **95**, 195135 (2017).
[18] A. Russomanno, F. Iemini, M. Dalmonte, and R. Fazio, Phys. Rev. B **95**, 214307 (2017).
[19] W. W. Ho, S. Choi, M. D. Lukin, and D. A. Abanin, Phys. Rev. Lett. **119**, 010602 (2017).
[20] B. Huang, Y.-H. Wu, and W. V. Liu, Phys. Rev. Lett. **120**, 110603 (2018).
[21] F. Iemini, A. Russomanno, J. Keeling, M. Schirò, M. Dalmonte, and R. Fazio, Phys. Rev. Lett. **121**, 035301 (2018).
[22] R. R. W. Wang, B. Xing, G. G. Carlo, and D. Poletti, Phys. Rev. E **97**, 020202(R) (2018).
[23] T.-S. Zeng and D. N. Sheng, Phys. Rev. B **96**, 094202 (2017).
[24] F. M. Surace, A. Russomanno, M. Dalmonte, A. Silva, R. Fazio, and F. Iemini, Phys. Rev. B **99**, 104303 (2019).
[25] K. Mizuta, K. Takasan, M. Nakagawa, and N. Kawakami, Phys. Rev. Lett. **121**, 093001 (2018).
[26] K. Giergiel, A. Kosior, P. Hannaford, and K. Sacha, Phys. Rev. A **98**, 013613 (2018).
[27] A. Kosior and K. Sacha, Phys. Rev. A **97**, 053621 (2018).
[28] A. Kosior, A. Syrwid, and K. Sacha, Phys. Rev. A **98**, 023612 (2018).
[29] A. Pizzi, J. Knolle, and A. Nunnenkamp, Phys. Rev. Lett. **123**, 150601 (2019).
[30] P. Liang, M. Marthaler, and L. Guo, New J. Phys. **20**, 023043 (2018).
[31] R. W. Bomantara and J. Gong, Phys. Rev. Lett. **120**, 230405 (2018).
[32] C. Fan, D. Rossini, H.-X. Zhang, J.-H. Wu, M. Artoni, and G. C. La Rocca, Phys. Rev. A **101**, 013417 (2020).
[33] V. K. Kozin and O. Kyriienko, Phys. Rev. Lett. **123**, 210602 (2019).
[34] P. Matus and K. Sacha, Phys. Rev. A **99**, 033626 (2019).
[35] A. Pizzi, J. Knolle, and A. Nunnenkamp, Nat. Commun. **12**, 2341 (2021).
[36] A. Syrwid, A. Kosior, and K. Sacha, Phys. Rev. Lett. **124**, 178901 (2020).
[37] A. Syrwid, A. Kosior, and K. Sacha, Phys. Rev. Research **2**, 032038(R) (2020).
[38] A. Russomanno, S. Notarnicola, F. M. Surace, R. Fazio, M. Dalmonte, and M. Heyl, Phys. Rev. Research **2**, 012003(R) (2020).
[39] K. Giergiel, T. Tran, A. Zaheer, A. Singh, A. Sidorov, K. Sacha, and P. Hannaford, New J. Phys. **22**, 085004 (2020).
[40] J. Wang, P. Hannaford, and B. J. Dalton, New J. Phys. **23**, 063012 (2021).
[41] A. Kuroś, R. Mukherjee, W. Golletz, F. Sauvage, K. Giergiel, F. Mintert, and K. Sacha, New J. Phys. **22**, 095001 (2020).
[42] J. Zhang, P. W. Hess, A. Kyprianidis, P. Becker, A. Lee, J. Smith, G. Pagano, I.-D. Potirniche, A. C. Potter, A. Vishwanath *et al.*, Nature (London) **543**, 217 (2017).
[43] S. Choi, J. Choi, R. Landig, G. Kucsko, H. Zhou, J. Isoya, F. Jelezko, S. Onoda, H. Sumiya, V. Khemani *et al.*, Nature (London) **543**, 221 (2017).
[44] S. Pal, N. Nishad, T. S. Mahesh, and G. J. Sreejith, Phys. Rev. Lett. **120**, 180602 (2018).
[45] J. Rovny, R. L. Blum, and S. E. Barrett, Phys. Rev. Lett. **120**, 180603 (2018).

[46] S. Autti, V. B. Eltsov, and G. E. Volovik, Phys. Rev. Lett. **120**, 215301 (2018).
[47] A. J. E. Kreil, H. Y. Musiienko-Shmarova, S. Eggert, A. A. Serga, B. Hillebrands, D. A. Bozhko, A. Pomyalov, and V. S. L'vov, Phys. Rev. B **100**, 020406(R) (2019).
[48] J. Rovny, R. L. Blum, and S. E. Barrett, Phys. Rev. B **97**, 184301 (2018).
[49] J. Smits, L. Liao, H. T. C. Stoof, and P. van der Straten, Phys. Rev. Lett. **121**, 185301 (2018).
[50] L. Liao, J. Smits, P. van der Straten, and H. T. C. Stoof, Phys. Rev. A **99**, 013625 (2019).
[51] S. Autti, P. J. Heikkinen, J. T. Mäkinen, G. E. Volovik, V. V. Zavjalov, and V. B. Eltsov, Nat. Mater. **20**, 171 (2021).
[52] L. Guo, M. Marthaler, and G. Schön, Phys. Rev. Lett. **111**, 205303 (2013).
[53] K. Sacha and D. Delande, Phys. Rev. A **94**, 023633 (2016).
[54] M. Mierzejewski, K. Giergiel, and K. Sacha, Phys. Rev. B **96**, 140201(R) (2017).
[55] E. Lustig, Y. Sharabi, and M. Segev, Optica **5**, 1390 (2018).
[56] K. Giergiel, A. Miroszewski, and K. Sacha, Phys. Rev. Lett. **120**, 140401 (2018).
[57] K. Giergiel, A. Kuroś, and K. Sacha, Phys. Rev. B **99**, 220303(R) (2019).
[58] K. Sacha and J. Zakrzewski, Rep. Prog. Phys. **81**, 016401 (2018).
[59] V. Khemani, R. Moessner, and S. L. Sondhi, arXiv:1910.10745.
[60] L. Guo and P. Liang, New J. Phys. **22**, 075003 (2020).
[61] K. Sacha, *Time Crystals* (Springer International Publishing, Switzerland, Cham, 2020), ISBN 978-3-030-52523-1, 10.1007/978-3-030-52523-1.
[62] S. Taie, H. Ozawa, T. Ichinose, T. Nishio, S. Nakajima, and Y. Takahashi, Sci. Adv. **1** (2015).
[63] A. Dauphin, M. Müller, and M. A. Martin-Delgado, Phys. Rev. A **93**, 043611 (2016).
[64] D. Leykam, A. Andreanov, and S. Flach, Adv. Phys. **3**, 1473052 (2018).
[65] M. Tylutki and P. Törmä, Phys. Rev. B **98**, 094513 (2018).
[66] S. Taie, T. Ichinose, H. Ozawa, and Y. Takahashi, Nat. Commun. **11**, 257 (2020).
[67] See Supplemental Material at http://link.aps.org/supplemental/10.1103/PhysRevLett.127.263003 for (i) the detailed derivation of the effective Hamiltonian, (ii) the spectrum of the finite Lieb lattice and the description of the numerical procedure identifying the Wannier states w_j, (iii) the extended analysis of the selection rules for nonvanishing simultaneous tunneling processes, and (iv) analysis of corrections to the secular Hamiltonian.
[68] A. Buchleitner, D. Delande, and J. Zakrzewski, Phys. Rep. **368**, 409 (2002).
[69] We use the gravitational units, but assume that the gravitational acceleration is given by $g/\sqrt{2}$.
[70] P. H. Richter, H. J. Scholz, and A. Wittek, Nonlinearity **3**, 45 (1990).
[71] M. P. Wojtkowski, Commun. Math. Phys. **126**, 507 (1990).
[72] L. Landau and E. Lifshitz, *Mechanics*, t. 1 (Elsevier Science, New York, 1982), ISBN 9780080503479.
[73] A. Lichtenberg and M. Lieberman, *Regular and Chaotic Dynamics*, Applied Mathematical Sciences (Springer-Verlag, Berlin, 1992), ISBN 9783540977452.
[74] M. Antonowicz, J. Phys. A **14**, 1099 (1981).
[75] Note that the localized character of the Wannier functions w_i makes it experimentally feasible to load the atoms into the eigenstates of the flat band of the noninteracting system in a similar way, as discussed in [26].
[76] C. Chin, R. Grimm, P. Julienne, and E. Tiesinga, Rev. Mod. Phys. **82**, 1225 (2010).